Linking the effective thermal conductivity of snow to its shear strength and density

Florent Domine,[1,2] Josué Bock,[1] Samuel Morin,[3] and Gérald Giraud[3]

Received 21 February 2011; revised 30 September 2011; accepted 4 October 2011; published 10 December 2011.

[1] The effective thermal conductivity of snow, k_{eff}, is a crucial climatic and environmental variable. Here, we test the intuition that k_{eff} is linked to microstructural and mechanical properties by attempting to relate k_{eff} to density ρ_{snow}, and to shear strength σ measured with a handheld shear vane. We performed 106 combined measurements of k_{eff}, ρ_{snow} and σ in the Alps, Svalbard, Arctic Alaska, and near the North Pole, covering essentially all snow types. We find a good correlation between k_{eff} and ρ_{snow} which is not significantly different from that of Sturm et al. (1997). The correlation between k_{eff} and a combination of σ and ρ_{snow} is stronger than with density alone. We propose an equation linking k_{eff} (W m^{-1} K^{-1}) ρ_{snow} (kg m^{-3}) and σ (Pa): $k_{eff} = 7.114\ 10^{-5}\ \rho_{snow}\ \sigma^{0.333} + 2.367\ 10^{-2}$. This equation places constraints on the calculation of k_{eff}, ρ_{snow} and σ in avalanche warning models where σ is a key variable. For our samples, we calculate σ from measured values of k_{eff} and ρ_{snow} using our equation and compare the value to that predicted by the French MEPRA avalanche warning model, which uses density and grain type as input data. MEPRA and the prediction of σ based on k_{eff} and ρ_{snow} agree within 8%. MEPRA agrees with observations within 11%. Calculating σ from density only yields values 55% lower than measured, showing the interest of using additional data to predict σ.

Citation: Domine, F., J. Bock, S. Morin, and G. Giraud (2011), Linking the effective thermal conductivity of snow to its shear strength and density, *J. Geophys. Res.*, *116*, F04027, doi:10.1029/2011JF002000.

1. Introduction

[2] A noteworthy snow property is its rather low thermal conductivity [*Sturm et al.*, 1997], which insulates the ground from the extreme temperatures encountered at high latitudes, limiting the extent of Arctic permafrost [*Zhang*, 2005] and facilitating the survival of subnivean species. The importance of the insulating power of snow to mankind is revealed by the fact that it appears to be the first snow property recorded in literature. Xenophon of Athens, in his writing *Anabasis* (book 4, section 4, translation by author) relates a winter military retreat in the mountains of Eastern Anatolia in 400 B.C. and reports: "But during the night, enormous amounts of snow fell, so that arms and men lying down were covered. […] There was great hesitation in getting up, because the snow was keeping the men lying down warm."

[3] The thermal conductivity of snow shows large variations, between 0.025 and 0.65 W m^{-1} K^{-1} [*Sturm et al.*, 1997], because of the changes in snow microstructure during snow metamorphism [*Domine et al.*, 2003; *Flin et al.*, 2003; *Schneebeli and Sokratov*, 2004]. Unfortunately, despite its obvious interest to climate, biological activity, and every day human life, our understanding of the processes governing the evolution of snow thermal conductivity is insufficient to allow confident prediction, because insufficient data are available on this variable. A few field experiments [*Morin et al.*, 2010; *Sturm and Johnson*, 1992; *Sturm et al.*, 2002a] and laboratory studies [*Lehning et al.*, 2002; *Schneebeli and Sokratov*, 2004] have shown that snow thermal conductivity could increase or decrease over time, depending on the temperature and temperature gradient in the snowpack, but those data do not cover the full range of metamorphic conditions encountered in nature.

[4] Heat transfer through snow is the result of several processes that include conduction through the interconnected ice grains, conduction through air in the pore space, latent heat transfer due to sublimation-condensation cycles, and ventilation due to thermal convection or air advection [*Domine et al.*, 2007b; *Sturm et al.*, 1997]. The effective thermal conductivity of snow, k_{eff}, regroups the first three processes. Laboratory studies often use insulated containers where the heat flux F and the temperature gradient ∇T are measured [*Schneebeli and Sokratov*, 2004], allowing the determination of k_{eff} using Fourier's law:

$$F = -k_{eff} \nabla T. \quad (1)$$

For field work, the heated needle probe technique is easier to use. A needle is inserted in the snow, where it is heated

[1] Laboratoire de Glaciologie et Géophysique de l'Environnement, CNRS-INSU/Université Joseph Fourier-Grenoble I, Saint-Martin-d'Hères, France.
[2] Takuvik International Laboratory, CNRS/Université Laval, Quebec, Quebec, Canada.
[3] Météo-France/CNRS, CNRM-GAME, CEN, St-Martin-d'Hères, France.

0148-0227/11/2011JF002000

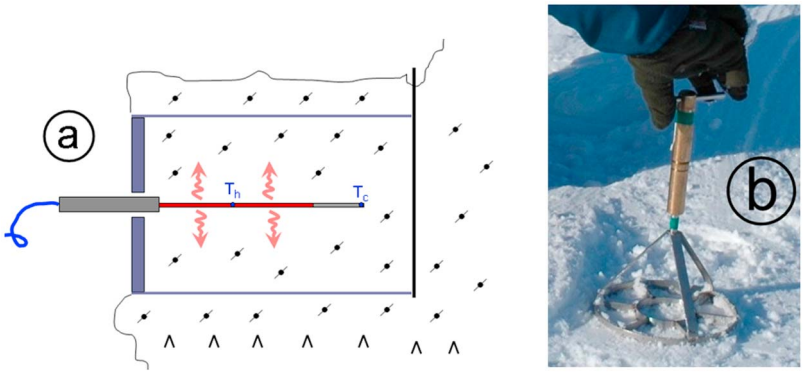

Figure 1. Experimental methods used. (a) For thermal conductivity measurements, a heated needle probe was inserted at the center of a tube to prevent ventilation during the measurement. The tube can be capped at both ends. The temperature difference T_h-T_c between a reference sensor and a sensor at the center of the heated zone is monitored to determine k_{eff}. (b) Shear vane used for shear strength measurements. It consists of six sharp radial vanes welded between two steel circles. The instrument is connected to a dynamometer. The handle is rotated and the dynamometer records the maximum torque applied when the snow shears.

with a known power for a period of time sufficient to mitigate the impact of the quality of thermal contact between the probe and the surrounding snow (Figure 1a). The rate of heating of the needle is inversely proportional to k_{eff}, and the monitoring of the temperature of the needle with time during heating allows the determination of k_{eff}. This is explained in the work by *Sturm et al.* [1997, and references therein], and a very detailed testing of the method has recently been performed by *Morin et al.* [2010].

[5] Many studies indicate that in most snow types the dominant process for heat transfer in snow is conduction through the interconnected ice grains [*Kaempfer et al.*, 2005; *Lehning et al.*, 2002; *Sturm et al.*, 1997] and this process is limited by the thickness of the bonds between the ice grains. It is therefore reasonable to seek a correlation between snow mechanical properties, also determined in part by bond size and strength, and thermal conductivity. In fact, previous studies have already assumed and confirmed a link between thermal conductivity and mechanical properties such as viscosity [*Fierz and Lehning*, 2001; *Lehning et al.*, 2002].

[6] Here, we investigate the link between the shear strength, σ, of the snow and k_{eff}. Shear strength can easily be measured in the field with a shear vane [*Brun and Rey*, 1987], shown in Figure 1b. For the purpose of this study, this lightweight and rapid instrument was a tool of choice to quantitatively estimate the shear strength of various snow types under many different snow and atmospheric conditions. We also measured snow density, as this variable is linked to both thermal conductivity and shear strength, albeit in a complex manner. Our objectives are twofold. First, we wish to test the hypothesis that the thermal conductivity of snow is mostly due to conduction throughout the interconnected network of ice crystals. To that end, we perform simultaneous measurements of k_{eff}, density and shear strength on snow of various types and seek physically relevant statistical linkages between these three variables. Second, we are interested in improving the internal consistency of models of snowpack evolution, which often predict thermal conductivity and shear strength independently. As a first test of current model links between both these variables, we compute the shear strength using the MEPRA model [*Durand et al.*, 1999] and compare the values obtained to our measurements.

2. Methods

2.1. Snowpacks Studied

[7] To study a large number of snow types, measurements were done during four consecutive winters from 2006 to 2009 in a large number of sites. In the French Alps, measurements were performed at Col de Porte, near Grenoble (1320 m asl, March 2007), just above Col du Lautaret (south facing, about 2100 m asl, February, March, and December 2008), and on a rocky outcrop on the edge of the Glacier du Bouchet (north facing, 3080 m asl, March 2007) accessible from the Orelle ski area. Snowpack types encountered were of the Alpine and maritime types, according to the classification of *Sturm et al.* [1995]. In Svalbard, measurements were performed in February and April 2006 near Ny-Ålesund, on the coastal wind-swept plain where the snowpack is of the tundra type, and on nearby glaciers (Austrebrøggerbreen and Comfortlessbreen) where the snowpack is Alpine. Further measurements were performed during the same periods on the East coast of Spitsbergen, on the sea ice in Ingelsfieldbukta, where the snowpack had essentially an Alpine character because of the unusual amounts of precipitation and warm temperatures in 2006. On the Arctic Ocean, measurements were performed around 88°N, 130°E in April 2007, near the frozen-in schooner TARA, during its 2006–2008 trans-Arctic drift [*Bottenheim et al.*, 2009]. The snowpack there essentially resembles the tundra snowpack, although it is much more variable and frozen crusts are frequent despite the fact that the temperature never rose above freezing. These crusts were caused by supercooled fog droplets generated by open leads that freeze upon contact with the snowpack. Finally, measurements were carried out around Barrow (Alaska north slope, 71°N, 157°E) in March 2009, mostly on land where the snowpack is of the tundra type, but also on the ocean within 1 km from the coast, where the snowpack was similar to that on land, although much more variable in thickness and on average a bit thinner.

[8] We made 55 measurements in Svalbard, 35 in the Alps, 7 near the North Pole and 9 in Alaska, totaling 106 measurements. In each case, a snow pit was dug, the stratigraphy was observed and recorded, the snow grain types were identified, then the measurements were made. Only layers sufficiently thick (≥4 cm) were studied, so that the three variables of interest could be measured reliably. Only dry snows were studied, but measurements on a large number of refrozen layers were performed.

2.2. Instrumentation

[9] The variable k_{eff} was measured with a TP02 needle probe from Hukseflux connected to a Campbell Scientific CR10X data logger. To prevent heat exchanges due to ventilation, a metal or plastic hollow cylinder 10 cm in diameter and 25 cm in length was inserted in the snow. A metal blade was placed snugly at the far end of the tube to prevent airflow through the tube. The TP02 needle was then inserted in the snow at the center of the tube, as shown in Figure 1a. In general, measurements were performed only when the wind was very light to light (estimated to be less than 4 m s^{-1}). However, at times, work had to be done in slightly stronger winds and a cap with a hole in its center was placed at the front end of the tube (Figure 1a). The system was thermally equilibrated for 5–10 min, which was almost always sufficient for the temperature of the needle probe to stabilize within ±0.2°C. In Barrow and at TARA, some measurements could be made in a tent where a large snow block containing the layer of interest was transported and thermally equilibrated for 5–18 h before measurements.

[10] The measurement sequence consisted of a 100 s baseline monitoring followed by 100 s of heating, with a power of 0.8 W, resulting in a temperature rise of 1.5–5 K. The temperature difference ΔT between the center of the 10 cm long heated region and the very end of the probe, 5 cm from the heated region, was monitored. In general, the temperature of the cold end of the needle probe did not vary by more than 0.12°C. Tests where the measurement was started before full thermal stabilization showed that this had little impact on the final result, because the variable of interest is the temperature difference between two sensors essentially subjected to the same variations, apart from the heating. The plot of ΔT versus ln(t), where t is time, showed a linear part, as detailed by *Sturm and Johnson* [1992] and *Morin et al.* [2010], whose slope is proportional to $1/k_{eff}$. Based on the analysis detailed by *Morin et al.* [2010], and on calibration with glycerol and polyurethane foam, we estimate that a k_{eff} value is accurate within 10%.

[11] As detailed by *Sturm and Johnson* [1992] and *Morin et al.* [2010], k_{eff} can be determined from both the heating and cooling parts of the curve, but the cooling part yields less accurate values [*Morin et al.*, 2010] so we only recorded the heating part. Because snow properties vary within a layer [*Matzl and Schneebeli*, 2006], and because shear strength measurements were repeated over about a 1 m wide area, the representativity of the k_{eff} values was checked by performing, in most cases, two to four measurements in the same layer. In over 80% of these cases, measurements in a given layer gave values within 10% of one another. When that was not the case, it was frequently because the layer was visibly inhomogeneous. The greatest heterogeneities were observed in layers subjected to melt-freeze cycles, where heterogeneous percolation, followed by re-freezing, caused significant variations at the cm scale. For heterogeneous layers, one of the two following strategies was followed. If time allowed, a large number of measurements (>6) was carried out to improve the statistical value of the average of the measurements, and the mean value was then taken as the k_{eff} of the layer. Variations from this mean sometimes reached 30%, illustrating the reality of heterogeneity in snow layers. If more measurements could not be performed, all data from that layer were discarded.

[12] Density was measured in the conventional manner by using density cutters and a field scale [*Conger and McClung*, 2009]. Cutters used were 500 and 100 cm^3 cylinders, and a 100 cm^3 box-type cutter. The cutter chosen depended on the layer thickness and hardness. For example, the 100 cm^3 box was used for hard windpacks while the 500 cm^3 tube was used for fresh or recent snow. *Conger and McClung* [2009] estimate that density measurements using such cutters have an accuracy of ±11%.

[13] Shear strength was measured with a shear vane as used by *Brun and Rey* [1987]. As shown in Figure 1b, it consists of a stainless steel wheel with six sharp radial vanes. It is placed firmly onto the surface of the snow layer, which had been cut flat with a sharp metal blade. The wheel is connected to a handle that is used to apply manually an increasing torque to the wheel, until the snow shears. The dynamometer that links the wheel to the handle indicates the maximum torque that has been applied, from which the shear strength σ is deduced. Wheels of three different diameters were used (7.6, 11.6, and 17.3 cm) for very hard snows (windpacks, melt-freeze layers), snows of medium hardness (fine grained snow, hard depth hoar), and soft snows (recent snow, depth hoar, layers of faceted crystals), respectively. Since shear measurements often show size effects [*Perla and Beck*, 1983], we tested this once by measuring shear strength on a snow layer using the large and medium wheels. A total of 2 × 10 measurements were made, with both average values within 8% of each other, the higher value being for the medium wheel. Since the difference was well within the uncertainty, no size correction was made.

[14] A manual shear vane as used is notorious for having a low reproducibility, in part because of natural variability in a snow layer, but also because the reading depends on the rotation speed, with fast rotations leading to values about 20% lower than slow ones. This observation is similar to that of *Perla and Beck* [1983], who observed that higher pull rates on a shear frame lowered shear strength values by 25%. *Perla and Beck* [1983] also noted that shear strength measurements were affected by the normal load applied to the frame. The only way to improve accuracy has been to increase the number of measurements while using a rotation speed as constant as possible, about 1 s for a 180° rotation, which we consider fast. Between 10 and 20 readings were taken for each layer studied [*Brun and Rey*, 1987]. This usually showed, once possible outliers had been removed, variations around the mean between ±20% for homogeneous layers and ±60% for heterogeneous layers. Efforts were also made to keep the normal load, applied by hand, constant. We applied reasonable pressure, probably equivalent to a weight of 2 or 3 kg, although this was not measured. We also investigated the handler's personal effect by having

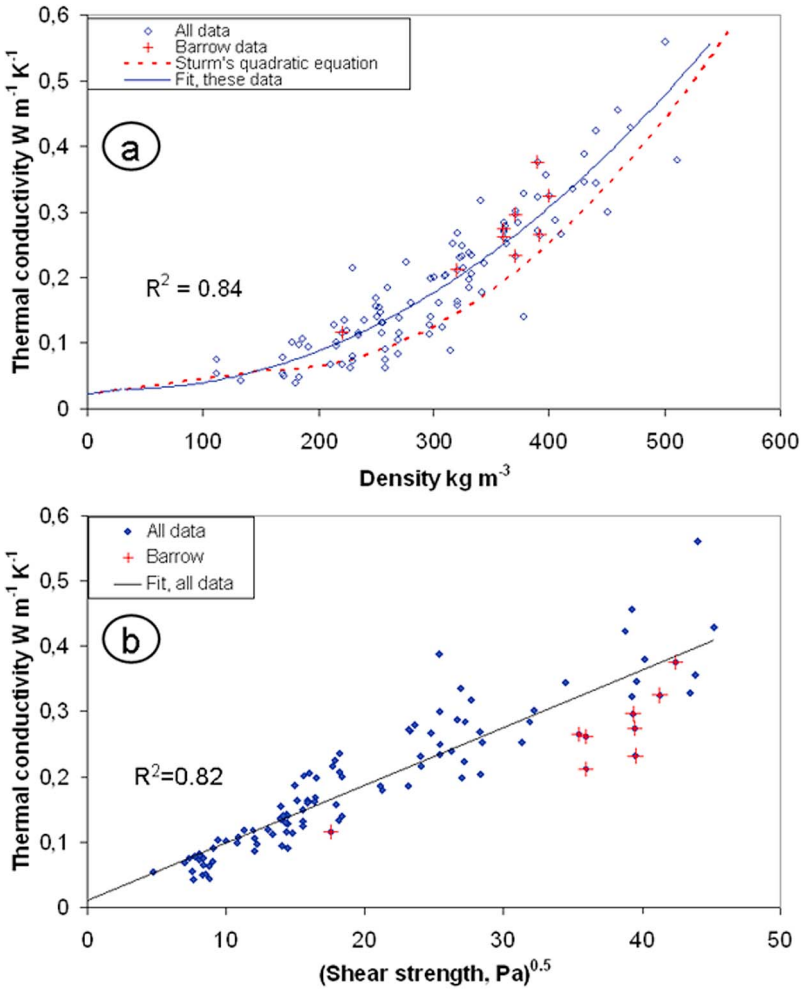

Figure 2. Relationship between the thermal conductivity of snow k_{eff} and (a) its density and (b) its (b) shear strength. The data obtained in Barrow have been singled out. For Figure 2a, the data have been fitted with a quadratic equation, with $R^2 = 0.84$. For comparison, the quadratic fit of *Sturm et al.* [1997] is also shown (dashed line). For Figure 2b, a linear fit having the thermal conductivity of air for $\rho = 0$ is shown.

the shear strength of a given layer measured by two people. We observed that a beginner tended to obtain higher values than an experienced handler, mostly because they tended to turn too slowly, but the difference decreased over time, to eventually stabilize to less than 10%. This 10% difference was not systematic, from which we deduce that the reading depended less on the handler, and was more random. We estimate that the random error of a shear strength measurement is about ±25%. An extra systematic error of up to ±20% is possible because of inadequate rotation speed or normal load, but we have not investigated this aspect in detail.

3. Results

[15] During our study of 106 snow layers, essentially all snow types (as classified by *Fierz et al.* [2009]) were encountered: precipitation particles (4 samples), decomposing or fragmented precipitation particles (18), rounded grains (14), windpacks (28), mixed forms; i.e., faceted rounded or rounding faceted particles (11), faceted crystals (11), depth hoar (10), melt-freeze layers, always studied refrozen (10). These 10 refrozen layers had undergone extensive melting, such that the original metamorphic crystal type prior to melting could not be recognized. Additionally, some of the layers entered in the other classes showed some light signs of melt-freeze cycling.

[16] We then sought empirical correlations between k_{eff} and the other physical properties measured. Figure 2a shows the correlation between k_{eff} and density ρ_{snow}. Similarly to *Sturm et al.* [1997], the data can be fitted well with a quadratic equation:

$$\begin{aligned} k_{eff} &= 2.041\ 10^{-6}\rho_{snow}{}^2 - 1.28\ 10^{-4}\rho_{snow} + 0.032 \\ &\qquad 30\ \text{kg m}^{-3} \le \rho_{snow} < 510\ \text{kg m}^{-3} \\ k_{eff} &= 2.37\ 10^{-4}\rho_{snow} + 0.0233 \\ &\qquad \rho_{snow} < 30\ \text{kg m}^{-3}, \end{aligned} \tag{2}$$

with k_{eff} in W m^{-1} K^{-1}. The first part of this equation is based on data in the density range 110 to 510 kg m^{-3}, with $R^2 = 0.84$. It can probably be extrapolated down to ρ_{snow} =

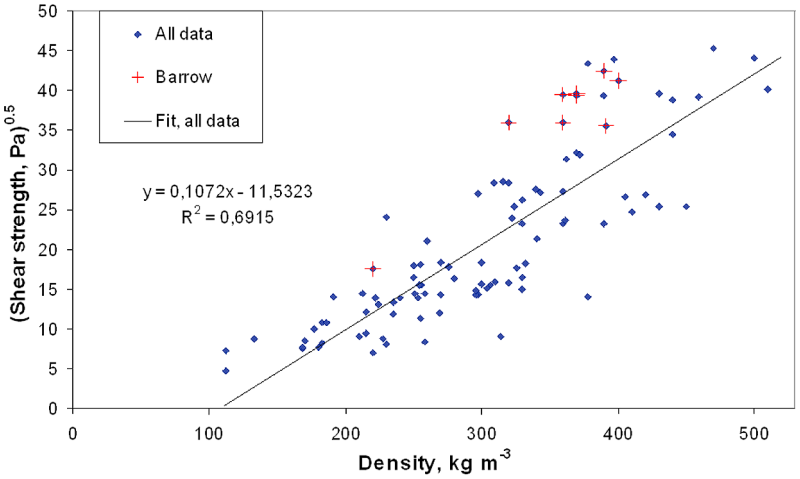

Figure 3. Relationships between the square root of the shear strength σ and density ρ. The data obtained in Barrow have been singled out. The linear fit of all the data is shown.

30 kg m^{-3}, giving k_{eff} = 0.0304 W m^{-1} K^{-1}, just slightly higher than the thermal conductivity of pure air (k_{air} = 0.0233 W m^{-1} K^{-1} at −10°C), and similar to the value predicted by the equation of *Sturm et al.* [1997]. In the rare occasions where lighter snow is encountered, a linear extrapolation to k_{eff} = 0.023 W m^{-1} K^{-1} for ρ_{snow} = 0 kg m^{-3} is recommended, as done by *Sturm et al.* [1997], and as done on the second line of equation (2). The root mean square deviation (RMSD) for this equation is 0.0223 W m^{-1} K^{-1}, showing a good reliability.

[17] Figure 2b investigates the correlation between k_{eff} and σ. Equations of the form $k_{eff} = \alpha\,\sigma^{\beta} + \gamma$ are convenient to use. The best correlation was obtained for the exponent β = 0.29 (R^2 = 0.84), but it makes sense to have k_{eff} close to the thermal conductivity of air for σ = 0. This latter criterion is best met when β = 0.53 (R^2 = 0.82), but to use simple exponents and since R^2 depends little on β, we used β = 0.5, yielding with σ in Pa and k_{eff} in W m^{-1} K^{-1}

$$k_{eff} = 0.00879\sigma^{0.5} + 0.01088, \tag{3}$$

with RMSD = 0.0286 W m^{-1} K^{-1}, showing that the prediction of k_{eff} from σ is slightly less accurate than that from ρ. Of course, there may be a large systematic error on σ, which this RMSD does not take into account.

[18] Similarly, Figure 3 shows the relationship between $\sigma^{0.5}$ and ρ, with R^2 = 0.69. It was found that lowering the exponent of σ improved the R^2 value, but the increase continued until the exponent neared zero, so that selecting the best exponent cannot be based on R^2, and has to be arbitrary if it is based on this graph. The equation, with σ in Pa and ρ in kg m^{-3} is

$$\sigma^{0.5} = 0.1072\,\rho - 11.53. \tag{4}$$

Here, the RMSD for predicting $\sigma^{0.5}$ is 4.02 Pa$^{0.5}$.

[19] We tested whether an empirical equation of the form $k_{eff} = \rho_{snow}^{\delta}\,\sigma^{\psi} + \nu$ could be a better predictor of k_{eff} than equations (2) or (3). The highest R^2 value for the linear regression of k_{eff} versus $\rho_{snow}^{\delta}\,\sigma^{\psi}$ was found for δ = 1.12 and ψ = 0.25 (R^2 = 0.909), but as above we also like to have $k_{eff} = k_{air}$ when ρ or σ = 0, and since also simple exponents are preferred, our best correlation is therefore

$$k_{eff} = 7.114\ 10^{-5}\rho_{snow}\sigma^{0.333} + 0.02367, \tag{5}$$

with k_{eff} in W m^{-1} K^{-1}, ρ_{snow} in kg m^{-3}, and σ in Pa. For equation (5), the R^2 value for the linear regression of k_{eff} versus $\rho_{snow}\,\sigma^{0.333}$ is 0.905. The RMSD is 0.0208 W m^{-1} K^{-1}, showing that equation (5) is the most reliable to predict k_{eff}.

[20] In Figure 4, we have used different symbols for each geographical area to show that the correlation does not depend on the location, with the notable exception of Barrow, where systematically lower k_{eff} values were found. Without the Barrow data, we find R^2 = 0.93.

4. Discussion

4.1. Comparison With the Literature

[21] Over a decade ago, *Sturm et al.* [1997] reviewed the data available at the time and summed up their own data, consisting in 488 values of k_{eff}, all obtained with a heated needle probe. From their data *Sturm et al.* [1997] proposed an equation (linear for ρ < 156 kg cm^{-3}, quadratic above) linking k_{eff} to density, which we reproduce in Figure 2. Since then, *Sturm et al.* [2002b] presented an additional series of 89 measurements from snow on sea ice. Subsequently, hardly any simultaneous measurements of k_{eff} and density have been published so we focus our discussion on the comparison with the data of *Sturm et al.* [1997].

[22] We thus compare the statistical distribution of the (ρ, k_{eff}) pairs obtained in this study and those presented by *Sturm et al.* [1997]. Based on 488 measurements of (ρ, k_{eff}) pairs, *Sturm et al.* [1997] derived a nonlinear regression law which one can use to compute an estimate $\hat{k}_{eff}$ of k_{eff} from the corresponding ρ value:

$$\hat{k}_{eff} = 0.138 - 1.01\ 10^{-3}\rho + 3.233\ 10^{-6}\rho^2 \text{ if } (156 \le \rho \le 600) \text{ kg m}^{-3}$$
$$\hat{k}_{eff} = 0.023 + 2.34\ 10^{-4}\rho \text{ if } \rho < 156 \text{ kg m}^{-3}. \tag{6}$$

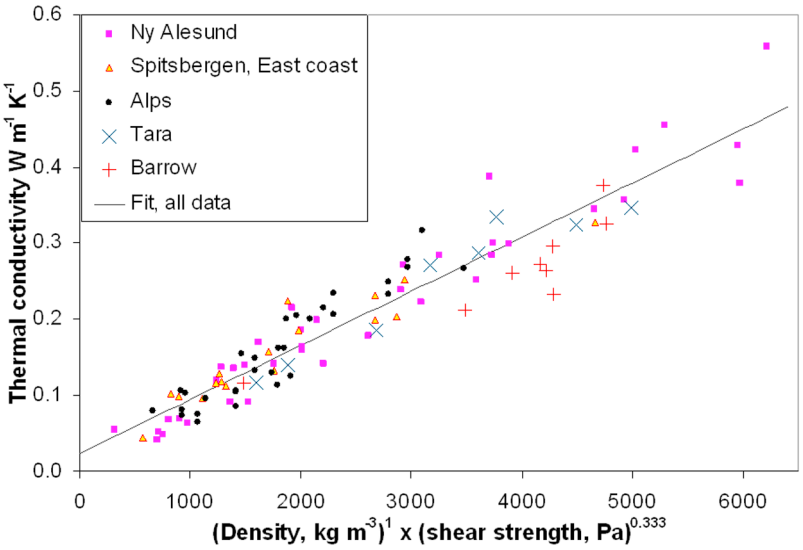

Figure 4. Relationship between the thermal conductivity of snow k_{eff} and the product of density ρ by the cubic root of shear strength σ. The geographical origin of the data is indicated, to show that all areas have the same trend, except Barrow. The linear correlation coefficient (equation (5)) for all the data is $R^2 = 0.905$.

We note κ the residual of the corresponding estimate of k_{eff}, i.e., for a given (ρ^i, k^i_{eff}) pair, $\kappa^i = \hat{k}^i_{eff} - k^i_{eff}$. The distribution of the 488 κ^i values obtained using all the (ρ, k_{eff}) pairs of *Sturm et al.* [1997] has an average value of 0.00 W m^{-1} K^{-1} and a standard deviation of 0.06 W m^{-1} K^{-1}. The distribution of the 106 κ^i values obtained using all the (ρ, k_{eff}) pairs of our study has an average value of 0.04 W m^{-1} K^{-1} and a standard deviation of 0.04 W m^{-1} K^{-1}. The Welch's t test applied to the two κ distributions demonstrates that their respective average values are statistically similar at the 99% confidence level. Conversely, if we apply the polynomial regression curve from our 106 (ρ, k_{eff}) pairs (equation (2)) to the *Sturm et al.* [1997] data set, the distribution of κ values computed using our data and that of *Sturm et al.* [1997] are similar at the 99% confidence level. This means that, in terms of (ρ, k_{eff}) pairs, the sampling of *Sturm et al.* [1997] and our data set statistically correspond to the sampling of the same population of (ρ, k_{eff}) pairs. Both samples are probably biased due to the different proportions between snowpack types and associated snow types, but the scatter around the (ρ, k_{eff}) regression curves is such that the impact of such biases is statistically insignificant. This demonstrates that our data set is as representative a subset of the distribution of (ρ, k_{eff}) pairs in nature as the larger data set of *Sturm et al.* [1997]. The same applies also to the data set of *Sturm et al.* [2002b].

[23] Table 1 details the fraction of snow types in this work and that of *Sturm et al.* [1997]. We also analyze the data of *Sturm et al.* [2002b]. The samplings, although representative, feature different proportions of snow types. *Sturm et al.* [1997, 2002a] studied a large proportion of depth hoar and windpacks, while we investigated a large fraction of fragmented precipitation particles, mixed forms, faceted crystals and rounded grains. *Sturm et al.* [1997, 2002a] therefore focused more on Arctic and subarctic snowpacks while most of our work was on Alpine snowpacks. Thus, equation (2) may be more suitable for Alpine snowpacks, while the equation of *Sturm et al.* [1997] may be more suitable for Arctic and subarctic snow.

[24] As suggested by *Sturm et al.* [1997] and many authors before and after them, it is obvious that better regression curves could be produced using snowpack type or snow type-specific regression curves. However, our data set is not big enough to provide a consistent new formulation. Along with many others [*Sturm et al.*, 2002a, and references therein], our study indicates that snow structure is an important factor to determine k_{eff}, in addition to density. *Sturm et al.* [1997] briefly considered the $k_{eff}-\rho_{snow}$ relationship of highly simplified snow models consisting of

Table 1. Overview of the Distribution of Snow Types Within the Sampling of *Sturm et al.* [1997, 2002a] and This Study[a]

	Total	Precipitation Particles	Mixed Forms	Rounded Grains	Rounded Grains–Wind Slab	Melt-Freeze Crust	Faceted Crystals	Depth Hoar
Sturm et al. [1997]	478	31 (6.5%)	26 (5.4%)	60 (12.6%)	165 (34.5%)	21 (4.4%)	0 (0%)	175 (36.6%)
Sturm et al. [2002a]	88	2 (2.3%)	0 (0.0%)	6 (6.8%)	47 (53.4%)	0 (0%)	0 (0%)	33 (37.5%)
This study	106	22 (20.8%)	11 (10.4%)	14 (13.2%)	28 (26.4%)	10 (9.4%)	11 (10.4%)	10 (9.4%)

[a]Precipitation particles and fragmented precipitation particles have been regrouped. Mixed forms regroup faceted rounded particles and rounding faceted particles of the classification of *Fierz et al.* [2009].

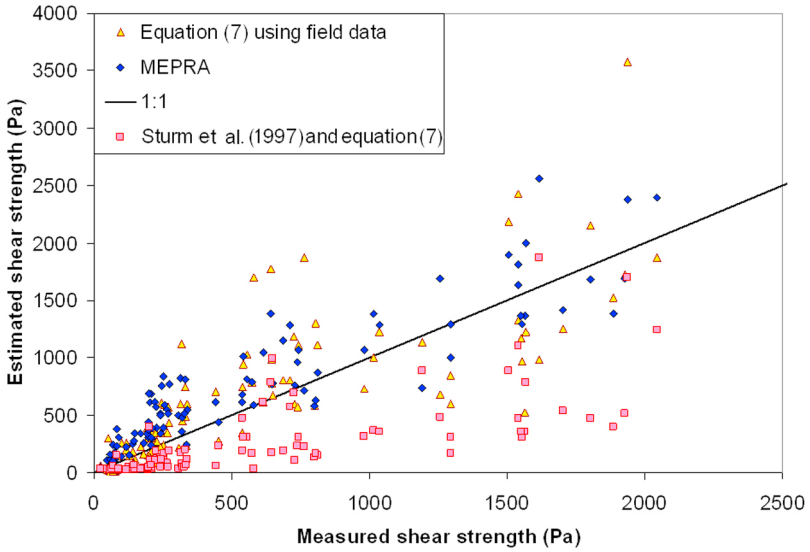

Figure 5. Comparison of three methods to estimate shear strength with field measurements: (1) inferred from equation (7) using field measurements of snow density and thermal conductivity; (2) with MEPRA, using measured snow density and observed snow grain type; and (3) inferred from measured density, thermal conductivity being calculated with the equation of *Sturm et al.* [1997] and equation (7).

plates of ice arranged either parallel or perpendicular to the heat flow, and by comparing the prediction of those models to their data, concluded that snow structure was not random, and that a more elaborate snow model might help determine relationships between grain size, bond size, and density in snow. Our data set is the first to combine measurements of a mechanical property, from which future modeling studies may derive information on bond strength.

4.2. The Case of the Barrow Snow

[25] Figures 2b and 4 show that the Barrow snow samples have systematically lower k_{eff} values than the general trend. Figure 2 shows that this is mostly due to an unusual k_{eff} -σ relationship, while the k_{eff} -ρ relationship is about normal. Figure 2b shows that σ for Barrow snow is about 30% greater than expected from its thermal conductivity. The first difference that comes to mind is the snow temperature, which was measured each time. In the Alps and Svalbard, the temperature was almost always warmer than −10°C. Near Tara, the temperature was around −15°C, and near Barrow the temperature was around −30°C. The effect of temperature on the shear vane response was investigated in the laboratory and showed no effect. It is possible that the lower temperature at Barrow reduced heat transfer through latent heat release. If that were the case, we expect the Barrow data to also stand out in the k_{eff} versus density plot in Figure 2a, but this is not observed. Figures 2b and 3 suggest either that some ice mechanical properties are temperature dependent or that Barrow snow has a different microstructure.

[26] There does not appear to be any study of the temperature dependence of the shear strength of snow. *Tusima* [1975] measured the hardness of snow between −2 and −56°C for several snow types, and found that hardness almost doubled between −10 and −30°C. More recently, *Schulson and Duval* [2009] reported a compilation of a related variable, fracture toughness of ice, which has units of Pa $m^{0.5}$, with measurements between −2 and −50°C. Most values show an error between 10 and 20%, but different studies show highly scattered values. For example, around −20°C, values range from 95 to 148 kPa $m^{0.5}$. It is therefore difficult to quantify a temperature trend in the fracture toughness, although the data suggest that this variable increases as temperature decreases. In conclusion, both publications indicate that mechanical properties of ice and snow increase at lower temperatures, and this effect may explain, fully or in part, the peculiar behavior of Barrow snow. We cannot, however, quantify the temperature dependence of snow shear strength from existing data so that other explanations are also worth exploring.

[27] While we were in Barrow, there was frequent precipitation and the snow was continuously remobilized by wind. As a result, the specific surface area of the snow which we measured by infrared reflectance [*Gallet et al.*, 2009] and whose values are reported elsewhere (F. Domine et al., Physical properties of the Arctic snowpack during OASIS, submitted to Journal of Geophysical Research, 2011) was unusually high; i.e., grains were small. Another suggestion to explain Barrow k_{eff} values is therefore that for a given density, the size of snow crystals and of bonds between grains was smaller; i.e., there was a larger number of smaller snow grains and of narrower bonds than for snows from other locations we studied. One way to look at this is that for a given k_{eff} value, heat conduction was taking place through a larger number of narrower bonds. We speculate that the shear strength is greater for a large number of thin bonds than for a small number of wide bonds, both configurations having the same cross-sectional surface area. If we are correct, we must conclude that there may be a number of climatic conditions where snow may behave somewhat differently from equation (5). More measurements in places such as the taiga or ice caps would be of interest to test the applicability of equation (5) to conditions not investigated here. Temperature effects should also be tested.

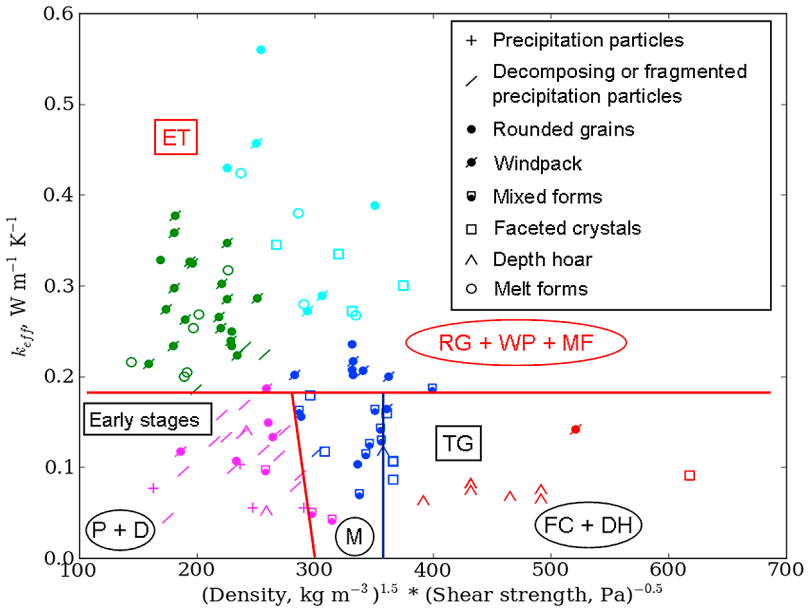

Figure 6. Graph to determine the metamorphic regime and snow type from values of k_{eff} and a combination of snow density and shear strength. The color of symbols show the result of a cluster analysis to attempt to regroup snow by type. Partly based on this analysis, an attempt has been made to define the domain of each snow type in the graph. The thick red lines define regions where the equi-temperature (ET) and temperature gradient (TG) regimes prevail. A region with low values of both variables characterize early stages of metamorphism, where the effect of the regime is not yet felt. In the ET regime, rounded grains (RG) and windpacks (WP) cannot be well separated. Refrozen melt forms (MF) also falls in this region. The early stages region concerns precipitation particles (P) and decomposing precipitation particles (D). The TG regions shows two domains. One is for mixed forms (M = faceting rounded crystals and rounding faceted crystals) and the other regroups faceted crystals (FC) and depth hoar (DH). From this graph, the group of snow types to which a sample belongs is determined correctly in 82% of cases.

4.3. Inferring Shear Strength From Thermal Conductivity

[28] One potentially promising outcome of the present work is the use of the link between thermal conductivity and shear strength in the context of snow avalanche prediction. Indeed, estimating the potential for accidental mechanical failure of the snowpack in a given slope requires, among other things, the knowledge of the vertical profile of the shear strength in the snowpack. The French operational model for avalanche risk evaluation estimates shear strength with the MEPRA submodel [*Durand et al.*, 1999]. The input data for MEPRA consists in a vertical profile of the physical properties of snow simulated with the snow physical model CROCUS [*Brun et al.*, 1992]. MEPRA then computes the mechanically relevant properties including shear strength. This computation is highly dependent on snow density, but also on snow grain type, which in CROCUS evolves with time in a discontinuous manner. MEPRA therefore predicts a discontinuous evolution of shear strength, whereas this is a continuous process in nature. In contrast, equation (5) can be used for a continuous description of shear strength as a function of density and effective thermal conductivity:

$$\sigma = \left(\frac{k_{eff} - 0.02367}{7.114 \times 10^{-5} \rho_{snow}} \right)^3. \quad (7)$$

We then tested the ability of various approaches to predict the shear strength of snow. In particular, it is of interest to evaluate the possibility to estimate shear strength from density only, given the correlation between σ and ρ_{snow} of Figure 3. Figure 5 uses our 106 measurements to compare the measured σ values to those predicted by three different methods: (1) equation (7), using the measured ρ_{snow} and k_{eff} values; (2) MEPRA using measured densities and observed snow types; (3) measured densities and the equation of *Sturm et al.* [1997] to predict k_{eff} from density, and then using the measured ρ_{snow} and the calculated k_{eff} to predict σ from equation (7). We chose the equation of *Sturm et al.* [1997] because it is the one based on the most data.

[29] Least square fits of the three approaches, forced through the origin, yield

$$\sigma_{\mathrm{eq(7)}} = 1.03 \times \sigma_{\mathrm{obs}} \; R^2 = 0.64 \quad (8)$$

$$\sigma_{\mathrm{MEPRA}} = 1.11 \times \sigma_{\mathrm{obs}} \; R^2 = 0.76 \quad (9)$$

$$\sigma_{\mathrm{eq(7)\ and\ Sturm}} = 0.45 \times \sigma_{\mathrm{obs}} \; R^2 = 0.54. \quad (10)$$

Both equation (7) with field data and MEPRA give reasonably good predictions of the measured shear strength. This is probably because both methods use both density and extra information to predict shear strength. In the case of equation (7), the extra information is the thermal conductivity, and in the case of MEPRA it is grain type. On the

other hand, if only density is used, in this case through the equation of *Sturm et al.* [1997], the lower amount of information leads to a less accurate prediction of shear strength. Also, since as shown in Figure 2a, the prediction of *Sturm et al.* [1997] gives lower k_{eff} values than this work, and since calculated σ values depend on k_{eff}^3, it is not surprising that significantly lower σ values are obtained in (10). In any case, Figure 5 shows the benefit of using more variables than just density to predict shear strength.

[30] We conclude that using equation (7) within a model requires finding a way to handle the time evolution of k_{eff} in a manner which explicitly relates to the evolution of the microstructure, and not mostly (if not only) based on density whose evolution is driven by snow compaction [e.g., *Brun et al.*, 1992; *Lehning et al.*, 2002]. If this is attained, an equation in the form of equation (7) can then be applied to estimate the shear strength, yielding results as good as MEPRA. To the best of our knowledge, existing snowpack models lack the required self-consistency in terms of microstructure representation to make full use of the relationship derived here.

4.4. Attempting to Classify Snow Using k_{eff}, ρ_{snow} and σ

[31] Recently, significant efforts have been devoted to the goal of determining unambiguously snow type from physical measurements, without having to resort to observations. *Marshall and Johnson* [2009] used measurements of snow mechanical properties with a SnowMicroPen to determine snow type. Although preliminary, their work shows a high success rate and appears quite promising. *Arakawa et al.* [2009] combined measurements of specific surface area and permeability to define well distinct domains for each snow type in the specific surface area-permeability diagram. To complement these studies, it is of interest to test whether our measurements can be used to contribute to an instrument-derived determination of snow type.

[32] Cluster analysis was used to test the possibility to determine snow type from our measurements. Briefly, a k-means clustering algorithm was used to identify groups of data points that are closest to each other in the space considered, while trying to maximize the distance between groups. This was attempted in 3D (k_{eff}, ρ, σ) and in 2D, using power combinations of the variables, as in Figure 4. In all cases, a given cluster was always made up of mostly one snow type, but there were always "alien" points within any cluster. In 2D, the most successful attempt was to plot k_{eff} versus $\rho_{snow}^{1.5} \times \sigma^{-0.5}$, as shown in Figure 6. (Note the negative power on σ, which is therefore markedly different from the expression used in Figure 4 and equation (5).) A color is used for each cluster and the symbols of *Fierz et al.* [2009] identify the snow type. Superimposed on this cluster analysis, we have attempted to draw boundaries for areas that would best characterize each snow type, while mostly respecting cluster domains. In this attempt, we found no good way to separate the areas between the green and cyan clusters, and to produce simple boundaries we have not fully respected clusters limits. The domains we propose are not perfect, and there is some overlap, just like in the figures of *Arakawa et al.* [2009], which show some degree of overlap between various snow types and metamorphic regimes. Nevertheless, this figure shows that the probability of determining the correct snow type is 82%.

[33] Figure 6 suggests that the metamorphic regime can be determined from the value of k_{eff}. Above 0.18 W m^{-1} K^{-1}, the regime is quasi-isothermal (Equi-Temperature, or ET according to *Sommerfeld and LaChapelle* [1970]) or significant melting took place, while below that value the snow evolved under a high Temperature Gradient (TG regime according to *Sommerfeld and LaChapelle* [1970]), or the snow is still in its initial stages of evolution. In the TG regime, the degree of evolution increases with the product $\rho_{snow}^{1.5} \times \sigma^{-0.5}$. Lower values characterize mixed forms, i.e., faceting rounded crystals or rounding faceting crystals, according to the classification of *Fierz et al.* [2009]. Faceted crystals and depth hoar are then observed with the highest values. We do not have enough data to separate faceted crystals from depth hoar. Likewise, in the ET regime, small rounded grains and windpacks cannot be well separated with the data available. Defining precisely the degree of overlap would also require more data, and identifying individually the error on each point would also be useful to establish the most reliable measurements. Other variables such as specific surface area, easily measured in the field using infrared reflectance [*Gallet et al.*, 2009], would be useful, in particular to distinguish refrozen layers from windpacks and small rounded grains, as melting leads to the lowest specific surface area values [*Domine et al.*, 2007a].

5. Conclusion

[34] Previous studies have shown a correlation between the thermal conductivity and the density of snow, and this correlation has been widely used, including in models of snowpack evolution. We confirm this correlation, but our data confirm that thermal conductivity also depends on microstructure. The originality of this work is to provide data on shear strength, a physical variable that can easily be measured in the field. We show here that by using shear strength in conjunction with density, the prediction of k_{eff} is improved. An added advantage of predicting k_{eff} from both density and shear strength is that it allows the verification of the internal consistency of snowpack models that predict these three variables. This is of particular interest for models used for avalanche prediction.

[35] We must however stress the current limitation of the relationship proposed here. The case of the Barrow data indeed may suggests that the 106 measurements performed here are not representative of all the snow types that can be encountered. It may also suggest that the shear strength dependence on temperature must be quantified.

[36] Measuring simultaneously thermal conductivity, density and shear strength helps in determining objectively snow type, but Figure 6 shows that this is not perfect. Additional data such as specific surface area (SSA) would probably improve snow type determination, in particular to detect melting. Furthermore, SSA may be useful to understand and predict thermal conductivity because latent heat transfer takes place at the surface of snow crystals.

[37] Last, efforts to understand the actual microstructural reasons for the relationships evidenced empirically here are warranted. The most rigorous way would be to obtain the three-dimensional structure of the snow samples by X-ray tomography, use numerical methods to calculate k_{eff} from these 3-D images, and compare them to measurements.

Preliminary attempts have already been made by *Kaempfer et al.* [2005], but they considered only heat transfer through the ice network, and neglected transfer through air and latent heat contributions. A more complete description of processes may be required to fully elucidate structure-properties relationships.

[38] **Acknowledgments.** Work in the Arctic was funded by the French Polar Institute (IPEV) through grant OSMAR437 (Svalbard), grant SMABASSI1051 (TARA), and grant OASIS1017 (Alaska) to F.D. The TARA measurements were also supported by the European commission through the DAMOCLES program, and F.D. thanks Jean-Claude Gascard for his invitation to come to TARA. Yves Lejeune (CNRM-GAME/CEN) kindly let us use his shear vane during all those years and provided the relevant training. Helpful discussions with Christian Geindreau (3S-R) on the mechanical properties of granular solids are acknowledged. Matthew Sturm (CRREL) kindly provided details of his data to allow the representativity tests. Constructive reviews by Matthew Sturm and two anonymous reviewers are acknowledged. We thank the Orelle ski area for providing free access and greatly facilitating our logistics in some of the finest Alpine scenery. We extend our gratitude to Eric Brossier and France Pincson du Sel for hosting us on board *Vagabond* on the East coast of Spitsbergen, and to Stefano Poli for competent guiding and for calmly handling bear attacks. Further help with logistics, some of the measurements and data handling were provided by many colleagues, including Marion Bisiaux, Frédéric Parrenin, Markus Frey, Xavier Fain at LGGE, Laurent Mérindol at CNRM-GAME/CEN, and IPEV field staff.

References

Arakawa, H., K. Izumi, K. Kawashima, and T. Kawamura (2009), Study on quantitative classification of seasonal snow using specific surface area and intrinsic permeability, *Cold Reg. Sci. Technol.*, *59*(2–3), 163–168, doi:10.1016/j.coldregions.2009.07.004.

Bottenheim, J. W., S. Netcheva, S. Morin, and S. V. Nghiem (2009), Ozone in the boundary layer air over the Arctic Ocean: Measurements during the TARA transpolar drift 2006–2008, *Atmos. Chem. Phys.*, *9*(14), 4545–4557, doi:10.5194/acp-9-4545-2009.

Brun, E., and L. Rey (1987), Field study on snow mechanical properties with special regard to liquid water content, in *Avalanche Gormation, Movement and Effects*, edited by B. Salm and H. Gubler, *IAHS Publ.*, *162*, 183–193.

Brun, E., P. David, M. Sudul, and G. Brunot (1992), A numerical-model to simulate snow-cover stratigraphy for operational avalanche forecasting, *J. Glaciol.*, *38*(128), 13–22.

Conger, S. M., and D. M. McClung (2009), Comparison of density cutters for snow profile observations, *J. Glaciol.*, *55*(189), 163–169, doi:10.3189/002214309788609038.

Domine, F., T. Lauzier, A. Cabanes, L. Legagneux, W. F. Kuhs, K. Techmer, and T. Heinrichs (2003), Snow metamorphism as revealed by scanning electron microscopy, *Microsc. Res. Tech.*, *62*(1), 33–48, doi:10.1002/jemt.10384.

Domine, F., A.-S. Taillandier, and W. R. Simpson (2007a), A parameterization of the specific surface area of seasonal snow for field use and for models of snowpack evolution, *J. Geophys. Res.*, *112*, F02031, doi:10.1029/2006JF000512.

Domine, F., A.-S. Taillandier, S. Houdier, F. Parrenin, W. R. Simpson, and T. A. Douglas (2007b), Interactions between snow metamorphism and climate: Physical and chemical aspects, in *Physics and Chemistry of Ice*, edited by W. F. Kuhs, pp. 27–46, R. Soc. of Chem., Cambridge, U. K.

Durand, Y., G. Giraud, E. Brun, L. Merindol, and E. Martin (1999), A computer-based system simulating snowpack structures as a tool for regional avalanche forecasting, *J. Glaciol.*, *45*(151), 469–484.

Fierz, C., and M. Lehning (2001), Assessment of the micro structure-based snow-cover model SNOWPACK: Thermal and mechanical properties, *Cold Reg. Sci. Technol.*, *33*(2–3), 123–131, doi:10.1016/S0165-232X(01)00033-7.

Fierz, C., R. L. Armstrong, Y. Durand, P. Etchevers, E. Greene, D. M. McClung, K. Nishimura, P. K. Satyawali, and S. A. Sokratov (2009), *The International Classification for Seasonal Snow on the Ground, IHP-VII Tech. Doc. Hydrol. 83, IACS Contrib. 1*, 80 pp., UNESCO-IHP, Paris.

Flin, F., J. B. Brzoska, B. Lesaffre, C. Cileou, and R. A. Pieritz (2003), Full three-dimensional modelling of curvature-dependent snow metamorphism: First results and comparison with experimental tomographic data, *J. Phys. D Appl. Phys.*, *36*(10A), 49–54, doi:10.1088/0022-3727/36/10A/310.

Gallet, J.-C., F. Domine, C. S. Zender, and G. Picard (2009), Measurement of the specific surface area of snow using infrared reflectance in an integrating sphere at 1310 and 1550 nm, *Cryosphere*, *3*(2), 167–182, doi:10.5194/tc-3-167-2009.

Kaempfer, T. U., M. Schneebeli, and S. A. Sokratov (2005), A microstructural approach to model heat transfer in snow, *Geophys. Res. Lett.*, *32*, L21503, doi:10.1029/2005GL023873.

Lehning, M., P. Bartelt, B. Brown, C. Fierz, and P. Satyawali (2002), A physical SNOWPACK model for the Swiss avalanche warning Part II: Snow microstructure, *Cold Reg. Sci. Technol.*, *35*(3), 147–167, doi:10.1016/S0165-232X(02)00073-3.

Marshall, H.-P., and J. B. Johnson (2009), Accurate inversion of high-resolution snow penetrometer signals for microstructural and micromechanical properties, *J. Geophys. Res.*, *114*, F04016, doi:10.1029/2009JF001269.

Matzl, M., and M. Schneebeli (2006), Measuring specific surface area of snow by near-infrared photography, *J. Glaciol.*, *52*(179), 558–564, doi:10.3189/172756506781828412.

Morin, S., F. Domine, L. Arnaud, and G. Picard (2010), In-situ measurement of the effective thermal conductivity of snow, *Cold Reg. Sci. Technol.*, *64*, 73–80, doi:10.1016/j.coldregions.2010.02.008.

Perla, R., and T. M. H. Beck (1983), Instruments and methods–Experience with shear frames, *J. Glaciol.*, *29*(103), 485–491.

Schneebeli, M., and S. A. Sokratov (2004), Tomography of temperature gradient metamorphism of snow and associated changes in heat conductivity, *Hydrol. Processes*, *18*(18), 3655–3665, doi:10.1002/hyp.5800.

Schulson, E. M., and P. Duval (2009), *Creep and Fracture of Ice*, 401 pp., Cambridge Univ Press, U. K., doi:10.1017/CBO9780511581397.

Sommerfeld, R. A., and E. LaChapelle (1970), The classification of snow metamorphism, *J. Glaciol.*, *9*(55), 3–17.

Sturm, M., and J. B. Johnson (1992), Thermal-conductivity measurements of depth hoar, *J. Geophys. Res.*, *97*(B2), 2129–2139, doi:10.1029/91JB02685.

Sturm, M., J. Holmgren, and G. E. Liston (1995), A seasonal snow cover classification-system for local to global applications, *J. Clim.*, *8*(5), 1261–1283, doi:10.1175/1520-0442(1995)008<1261:ASSCCS>2.0.CO;2.

Sturm, M., J. Holmgren, M. Konig, and K. Morris (1997), The thermal conductivity of seasonal snow, *J. Glaciol.*, *43*(143), 26–41.

Sturm, M., D. K. Perovich, and J. Holmgren (2002a), Thermal conductivity and heat transfer through the snow on the ice of the Beaufort Sea, *J. Geophys. Res.*, *107*(C21), 8043, doi:10.1029/2000JC000409.

Sturm, M., J. Holmgren, and D. K. Perovich (2002b), Winter snow cover on the sea ice of the Arctic Ocean at the Surface Heat Budget of the Arctic Ocean (SHEBA): Temporal evolution and spatial variability, *J. Geophys. Res.*, *107*(C10), 8047, doi:10.1029/2000JC000400.

Tusima, K. (1975), The temperature dependence of hardness of snow, in *Snow Mechanics*, edited by J. Nye, *IAHS Publ.*, *114*, 103–109.

Zhang, T. J. (2005), Influence of the seasonal snow cover on the ground thermal regime: An overview, *Rev. Geophys.*, *43*, RG4002, doi:10.1029/2004RG000157.

J. Bock, Laboratoire de Glaciologie et Géophysique de l'Environnement, CNRS-INSU/Université Joseph Fourier-Grenoble I, BP 96, F-38402 St-Martin-d'Hères CEDEX, France.

F. Domine, Takuvik International Laboratory, CNRS/Université Laval, 1045 avenue de la Médecine, Quebec QC, G1V 0A6, Canada. (florent.domine@gmail.com)

G. Giraud and S. Morin, Météo-France/CNRS, CNRM-GAME, CEN, F-38402 St-Martin-d'Hères CEDEX, France.